



HAL
open science

High-pressure phases of $\text{Tb}_2\text{Ni}_2\text{Sn}$ and $\text{Dy}_2\text{Ni}_2\text{Sn}$

Gunter Heymann, Birgit Heying, Ute Ch. Rodewald, Bernard Chevalier,
Hubert Huppertz, Rainer Pöttgen

► **To cite this version:**

Gunter Heymann, Birgit Heying, Ute Ch. Rodewald, Bernard Chevalier, Hubert Huppertz, et al.. High-pressure phases of $\text{Tb}_2\text{Ni}_2\text{Sn}$ and $\text{Dy}_2\text{Ni}_2\text{Sn}$. *Chemical Monthly = Monatshefte für Chemie*, 2014, 145 (6), pp.863-867. 10.1007/s00706-014-1179-8 . hal-00990899

HAL Id: hal-00990899

<https://hal.science/hal-00990899>

Submitted on 13 Jul 2022

HAL is a multi-disciplinary open access archive for the deposit and dissemination of scientific research documents, whether they are published or not. The documents may come from teaching and research institutions in France or abroad, or from public or private research centers.

L'archive ouverte pluridisciplinaire **HAL**, est destinée au dépôt et à la diffusion de documents scientifiques de niveau recherche, publiés ou non, émanant des établissements d'enseignement et de recherche français ou étrangers, des laboratoires publics ou privés.

High-pressure phases of $\text{Tb}_2\text{Ni}_2\text{Sn}$ and $\text{Dy}_2\text{Ni}_2\text{Sn}$

Gunter Heymann · Birgit Heying · Ute Ch. Rodewald ·
Bernard Chevalier · Hubert Huppertz · Rainer Pöttgen

Abstract The $\text{W}_2\text{B}_2\text{Co}$ -type ternary stannides $\text{Tb}_2\text{Ni}_2\text{Sn}$ and $\text{Dy}_2\text{Ni}_2\text{Sn}$ (space group $Immm$) show pressure-induced reconstructive phase transitions. Under high-pressure (8 GPa) and high-temperature (1,470 K) treatment they transform to the tetragonal $\text{Mo}_2\text{B}_2\text{Fe}$ -type high-pressure (HP) modifications: $P4/mbm$, $a = 732.6(1)$ pm, $c = 371.71(9)$ pm, $wR2 = 0.0319$, 225 F^2 values for HP- $\text{Tb}_2\text{Ni}_2\text{Sn}$ and $a = 730.3(2)$ pm, $c = 369.1(2)$ pm, $wR2 = 0.0221$, 230 F^2 values for HP- $\text{Dy}_2\text{Ni}_2\text{Sn}$, with 12 variables per refinement. At 8 GPa HP- $\text{Tb}_2\text{Ni}_2\text{Sn}$ and HP- $\text{Dy}_2\text{Ni}_2\text{Sn}$ started to decompose into the equiatomic stannides TbNiSn and DyNiSn and a yet unknown phase. Single-crystal diffractometry revealed the following data: TiNiSi type, $Pnma$, $a = 714.9(1)$ pm, $b = 445.9(1)$ pm, $c = 766.4(1)$ pm, $wR2 = 0.0558$, 575 F^2 values, 20 parameters for TbNiSn and $a = 710.5(1)$ pm, $b = 445.31(9)$ pm, $c = 765.7(1)$ pm for DyNiSn . The cell volumes of HP- $\text{Tb}_2\text{Ni}_2\text{Sn}$ and HP- $\text{Dy}_2\text{Ni}_2\text{Sn}$ nicely fit into the Iandelli plot of the whole $\text{RE}_2\text{Ni}_2\text{Sn}$ (RE = rare earth) series of compounds. The polyanionic networks $[\text{NiSn}]$ and $[\text{Ni}_2\text{Sn}]$ of the investigated ternary stannides show covalent Ni–Sn bonding with distorted tetrahedral $\text{SnNi}_{4/4}$ coordination

(259–279 pm Ni–Sn) in the RENiSn compounds and a square-planar $\text{SnNi}_{4/4}$ arrangement (291–292 pm Ni–Sn) in HP- $\text{Tb}_2\text{Ni}_2\text{Sn}$ and HP- $\text{Dy}_2\text{Ni}_2\text{Sn}$. The nickel atoms form Ni_2 pairs with Ni–Ni distances of 250 pm.

Keywords Ternary stannides · High-pressure phase · Intermetallics

Introduction

The series of $\text{RE}_2\text{Ni}_2\text{Sn}$ ternary stannides shows dimorphism. The larger rare earth (RE) elements Ce, Pr, Nd, Sm, Gd, Tb, Dy, and Y form the orthorhombic $\text{W}_2\text{B}_2\text{Co}$ -type structure, space group $Immm$, whereas the smaller ones with Ho, Er, Tm, Lu, and Sc lead to the tetragonal $\text{Mo}_2\text{B}_2\text{Fe}$ structure, space group $P4/mbm$. The crystal chemical data of this series are summarized in Ref. [1]. The common structural motifs of both structures are nickel-centered trigonal prisms which show different condensation patterns.

The interesting point in such dimorphic series concerns the break in structure type. The latter is mostly a consequence of the size of the RE atom (lanthanoid contraction). At a critical size a given structure type is no longer feasible and there are three ways out: (a) the series of compounds ends with that RE element, (b) the structure shows superstructure formation with a well-defined group–subgroup relation, or (c) a reconstructive phase transition to a different structure type but with the same composition occurs [2]. This last version is the case for the $\text{RE}_2\text{Ni}_2\text{Sn}$ series.

At the transition point it is sometimes possible to stabilize metastable phases. The compound with the first RE element of the new structure type might form the previous structure type as a high-temperature phase that can be

G. Heymann · H. Huppertz
Institut für Allgemeine, Anorganische und Theoretische Chemie,
Leopold-Franzens-Universität Innsbruck, Innrain 80-82,
6020 Innsbruck, Austria

B. Heying · U. Ch. Rodewald · R. Pöttgen (✉)
Institut für Anorganische und Analytische Chemie, Westfälische
Wilhelms-Universität Münster, Corrensstrasse 30,
48149 Münster, Germany
e-mail: pottgen@uni-muenster.de

B. Chevalier
CNRS, Université de Bordeaux, ICMCB, 87 Avenue
Dr. A. Schweitzer, 33608 Pessac Cedex, France

quenched in the case of a reconstructive phase transition. In contrast, the last representative of a series might form a high-pressure (HP) phase with the other structure type. In the field of intermetallics we succeeded in stabilizing such phases in the series of RENiSn, REPdSn, and REAgSn stannides [3, 4]. We have now tested the W₂B₂Co-type ternary stannides Tb₂Ni₂Sn and Dy₂Ni₂Sn under similar high-pressure high-temperature conditions and could stabilize the new high-pressure phases HP-Tb₂Ni₂Sn and HP-Dy₂Ni₂Sn with Mo₂B₂Fe-type structure. The synthesis conditions, structure determinations, and crystal chemical details are reported herein.

Results and discussion

Structure refinements

Analyses of the X-ray single-crystal diffractometer data sets showed that both specimens consisted of large domains of the HP-Tb₂Ni₂Sn and HP-Dy₂Ni₂Sn phases and very small domains (around 5 %) of the decomposition products TbNiSn and DyNiSn. Consequently we integrated two separate data sets for each crystal. The TbNiSn and DyNiSn data sets showed primitive orthorhombic lattices (Table 1) and the systematic extinctions were compatible with space group *Pnma*, in agreement with earlier work on CeNiSn [3]. The positional parameters of the cerium compound were taken as starting values. The HP-Tb₂Ni₂Sn and HP-Dy₂Ni₂Sn data sets showed primitive tetragonal lattices and the systematic extinctions were in accordance with space group *P4/mbm*, similar to Ho₂Ni₂Sn [1]. Consequently we used the positional parameters of Ho₂Ni₂Sn as starting values. The four structures were then refined using SHELXL-97 [5, 6] (full-matrix least-squares on F^2) with anisotropic displacement parameters for all atoms. The

Table 1 Lattice parameters of TbNiSn, DyNiSn, HP-Tb₂Ni₂Sn, and HP-Dy₂Ni₂Sn

Compound	<i>a</i> /pm	<i>b</i> /pm	<i>c</i> /pm	<i>V</i> /nm ³	Reference
TbNiSn	714.9(1)	445.9(1)	766.4(1)	0.2443	This work
TbNiSn	714.6	444.8	766.1	0.2435	[7]
TbNiSn	713.8(3)	445.0(2)	766.0(3)	0.2433	[8]
TbNiSn	702.2	442.5	762.6	0.2370	[9]
DyNiSn*	710.5(1)	445.31(9)	765.7(1)	0.2423	This work
DyNiSn	711.2	443.9	765.6	0.2417	[7]
DyNiSn	712.1	445.6	766.0	0.2431	[2]
DyNiSn	708.8(2)	443.5(2)	765.5(3)	0.2406	[8]
HP-Tb ₂ Ni ₂ Sn	732.6(1)	<i>a</i>	371.71(9)	0.1995	This work
HP-Dy ₂ Ni ₂ Sn	730.3(2)	<i>a</i>	369.1(2)	0.1968	This work

* Single-crystal diffractometer data

lower quality of the DyNiSn data set (the domain size was very small; this led to weak overall intensities) allowed only for an anisotropic refinement of the Dy atoms. Nevertheless, we could prove its TiNiSi-type structure, but with bad residuals. These data are not listed here, but were deposited in a national crystallography database (*vide infra*).

Refinements of the occupancy parameters gave no hint for deviations from the ideal compositions. The refinements went smoothly to the values listed in Table 2. The final difference-Fourier syntheses revealed no significant residues. The refined atomic positions, isotropic displacement parameters, and interatomic distances are given in Tables 3 and 4, respectively.

Crystal chemistry

High-pressure and high-temperature experiments on W₂B₂Co-type Tb₂Ni₂Sn and Dy₂Ni₂Sn led to reconstructive phase transitions to HP-Tb₂Ni₂Sn and HP-Dy₂Ni₂Sn

Table 2 Crystal data and structure refinement results for HP-Tb₂Ni₂Sn, TbNiSn, and HP-Dy₂Ni₂Sn

Compound	HP-Tb ₂ Ni ₂ Sn	TbNiSn	HP-Dy ₂ Ni ₂ Sn
Structure type	Mo ₂ B ₂ Fe	TiNiSi	Mo ₂ B ₂ Fe
Unit cell dimensions	Table 1	Table 1	Table 1
Space group	<i>P4/mbm</i>	<i>Pnma</i>	<i>P4/mbm</i>
<i>Z</i>	2	4	2
Molar mass/g mol ⁻¹	553.95	336.32	561.11
Calculated density/g cm ⁻³	9.22	9.14	9.47
Absorption coefficient/mm ⁻¹	50.2	46.0	52.9
<i>F</i> (000)/e	472	572	476
Crystal size/μm ³	20 × 30 × 60	20 × 30 × 60	10 × 20 × 30
Transm. ratio (min/max)	0.101/0.475	0.293/0.658	0.191/0.600
θ range/°	3–33	3–35	3–33
Range in <i>hkl</i>	±11, ±11, ±5	±11, ±6, ±12	±11, ±11, ±5
Total no. reflections	2,553	2,901	2,393
Independent reflections/ <i>R</i> _{int}	225/0.1394	575/0.0503	230/0.0397
Reflections with $I \geq 2\sigma(I)/R_\sigma$	223/0.0530	492/0.0274	212/0.0186
Data/parameters	225/12	575/20	230/12
Goodness-of-fit on F^2	0.902	1.117	1.001
<i>R</i> ₁ / <i>wR</i> ₂ for [$I \geq 2\sigma(I)$]	0.0403/0.0310	0.0241/0.0511	0.0125/0.0219
<i>R</i> ₁ / <i>wR</i> ₂ for all data	0.0474/0.0319	0.0326/0.0558	0.0143/0.0221
Extinction coefficient	0.0044(5)	0.0040(4)	0.0085(4)
Largest diff. peak and hole/eÅ ⁻³	2.07/−1.90	2.54/−2.84	1.09/−0.79

Table 3 Atomic coordinates and equivalent isotropic displacement parameters/pm² of HP-Tb₂Ni₂Sn, TbNiSn, and HP-Dy₂Ni₂Sn

Atom	Wyck.	x	y	z	U_{eq}/U_{iso}
HP-Tb ₂ Ni ₂ Sn					
Tb	4h	0.17580(3)	$x + 1/2$	1/2	74(1)
Ni	4g	0.37915(9)	$x + 1/2$	0	111(2)
Sn	2a	0	0	0	83(2)
TbNiSn					
Tb	4c	0.01175(4)	1/4	0.70253(4)	70(1)
Ni	4c	0.3010(1)	1/4	0.4150(1)	96(2)
Sn	4c	0.19108(6)	1/4	0.08665(6)	67(1)
HP-Dy ₂ Ni ₂ Sn					
Dy	4h	0.17545(2)	$x + 1/2$	1/2	154(1)
Ni	4g	0.37918(7)	$x + 1/2$	0	188(2)
Sn	2a	0	0	0	162(1)

U_{eq} is defined as one-third of the trace of the orthogonalized U_{ij} tensor

with the tetragonal Mo₂B₂Fe structure. Similar experiments on Gd₂Ni₂Sn resulted in a new phase with a yet unknown structure. Most likely the gadolinium atoms are too large to enable formation of the tetragonal phase. Investigations on this new phase are in progress.

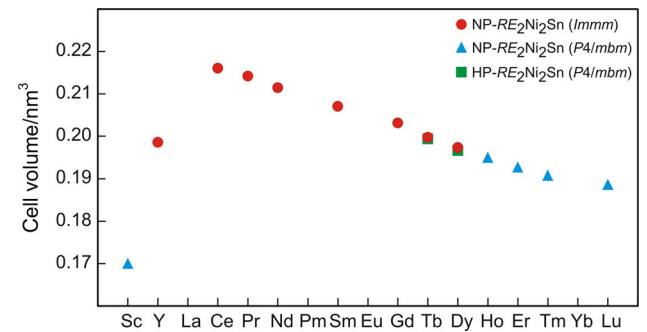
In Fig. 1 we present the course of the cell volumes within the RE₂Ni₂Sn series. HP-Tb₂Ni₂Sn and HP-Dy₂Ni₂Sn nicely extend the tetragonal RE₂Ni₂Sn (NP-RE₂Ni₂Sn, *P4/mbm*) ternary stannides towards the larger rare earth elements. The cell volumes are in agreement with the lanthanoid contraction. Both high-pressure phases show slightly smaller cell volumes. Nevertheless, direct comparison of absolute values is difficult, because the structure type changes as a consequence of the reconstructive phase transition.

A projection of the HP-Tb₂Ni₂Sn structure is presented in Fig. 2. It is best described (from a geometrical point of view) as an intergrowth variant of slightly distorted AIB₂ and CsCl related slabs of compositions TbNi₂ and TbSn. Together, the Ni₂ pairs and the Sn atoms form planar [Ni₂Sn] networks with distances of 250 pm for Ni–Ni and 292 pm for Ni–Sn, leading to SnNi_{4/4} square-planar coordination for the Sn atoms. The Ni–Sn contacts are only of weakly bonding character because they are much longer than the sum of the covalent radii of 255 pm [10]. Significant bonding contributions arise from Tb–Ni with comparatively short distances of 281 and 289 pm (Table 4). HP-Tb₂Ni₂Sn and HP-Dy₂Ni₂Sn belong to the large family of compounds with ordered U₃Si₂-type structure (Mo₂B₂Fe-type) and they are the first high-pressure representatives. The crystal chemistry and the bonding peculiarities of these intermetallics have been reviewed [11]. For further details we refer to this write-up as well as to the work on the normal-pressure NP-RE₂Ni₂Sn phases [1].

Table 4 Interatomic distances/pm, calculated with the powder lattice parameters of HP-Tb₂Ni₂Sn and TbNiSn

HP-Tb ₂ Ni ₂ Sn				TbNiSn			
Tb	2	Ni	280.9	Tb	1	Ni	302.2
	4	Ni	288.8		2	Ni	306.8
	4	Sn	327.9		2	Sn	311.2
	1	Tb	364.3		1	Sn	318.9
	2	Tb	371.7		2	Sn	320.5
	4	Tb	382.1		1	Sn	321.1
Ni	1	Ni	250.4		2	Ni	328.3
	2	Tb	280.9		1	Ni	329.6
	4	Tb	288.8		2	Tb	364.8
	2	Sn	291.5		2	Tb	382.6
Sn	4	Ni	291.5	Ni	2	Sn	259.0
	8	Tb	327.9		1	Sn	263.6
					1	Sn	278.9
					1	Tb	302.2
					2	Tb	306.8
					2	Tb	328.3
					1	Tb	329.6
				Sn	2	Ni	259.0
					1	Ni	263.6
					1	Ni	278.9
					2	Tb	311.2
					1	Tb	318.9
					2	Tb	320.5
					1	Tb	321.1

All distances within the first coordination spheres are listed. Standard deviations are all equal to or less than 0.3 pm

**Fig. 1** Cell volumes of normal-pressure (NP) and high-pressure (HP) phases in the series of RE₂Ni₂Sn ternary stannides

The high-pressure synthesis experiments indicated decomposition of the HP-RE₂Ni₂Sn phases towards higher pressures. Indeed, the terbium-containing sample already showed a considerable amount of equiatomic TbNiSn in the Guinier powder pattern and we were able to refine the lattice parameters (Table 1). Only traces of DyNiSn have been observed for the HP-Dy₂Ni₂Sn sample and the lattice

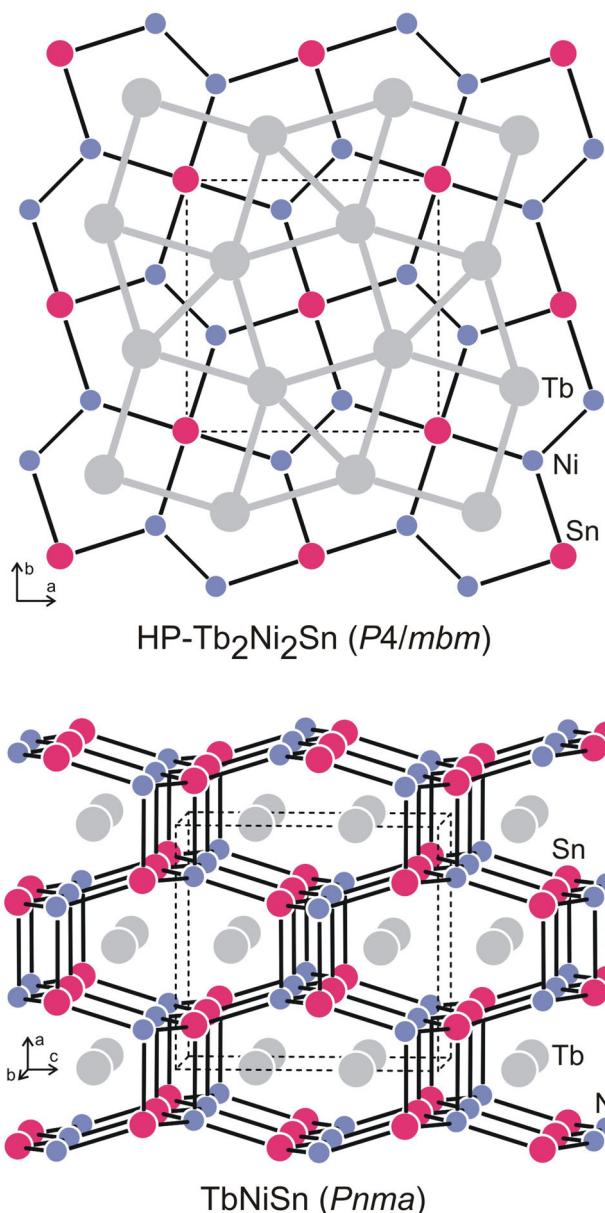


Fig. 2 Crystal structures of HP-Tb₂Ni₂Sn (Mo₂B₂Fe-type) and TbNiSn (TiNiSi-type)

parameters listed in Table 1 rely on the single-crystal diffractometer data. Since both single crystals showed tiny secondary domains, we could also refine the structures of TbNiSn and DyNiSn. So far, these two stannides had only been studied on the basis of powder X-ray diffraction [2, 7–9].

For comparison with HP-Tb₂Ni₂Sn we discuss the TbNiSn structure. Its TiNiSi-type unit cell is presented in Fig. 2. The Ni and Sn atoms form puckered Ni₃Sn₃ hexagons with distances of 259 and 264 pm for Ni–Sn, slightly longer than the sum of the covalent radii. Between the layers the Ni–Sn distances of 279 pm are even longer and thus the inter-layer Ni–Sn interactions are weaker. Such transition metal–tin distances typically occur in shandite

structures as well [12]. Within the three-dimensional [NiSn] network the Sn atoms have elongated tetrahedral SnNi_{4/4} coordination, in contrast to the planar arrangement in HP-Tb₂Ni₂Sn. The Ni–Sn distances are all shorter than in HP-Tb₂Ni₂Sn, indicating stronger overall Ni–Sn bonding in the equiatomic phase.

The Tb atoms are coordinated to two puckered and tilted Ni₃Sn₃ hexagons. This motif resembles the well-known AlB₂-type and consequently we can describe TbNiSn as an orthorhombically distorted ordering variant of AlB₂ [13]. More detailed crystal chemical discussion on TiNiSi-type intermetallics is available elsewhere [13–15]. The Tb atoms bind to the three-dimensional [NiSn] network via Tb–Ni contacts with Tb–Ni distances of 302 and 307 pm, longer than in HP-Tb₂Ni₂Sn. We can thus conclude that stronger Tb–Ni bonding exists in HP-Tb₂Ni₂Sn but stronger Ni–Sn bonding exists in TbNiSn. The same holds true for the isotopic dysprosium stannides.

Experimental

Synthesis of precursor compounds

Starting materials for the synthesis of the precursor ternary stannides Tb₂Ni₂Sn and Dy₂Ni₂Sn were pieces of terbium and dysprosium (Smart Elements), nickel wire (Alfa Aesar, Ø 1 mm), and tin granules (Merck, >4 mm), all with stated purities better than 99.9 %. The elements were weighed in the ideal 2:2:1 atomic ratio and first arc-melted [16] under an argon pressure of ca. 700 mbar. The buttons were remelted twice to ensure homogeneity. These arc-melted samples contained small amounts of an impurity phase. They were subsequently sealed in evacuated silica ampoules and annealed at 1,070 K for 1 week. The polycrystalline products are stable in air over months.

High-pressure high-temperature treatment

To obtain the tetragonal Mo₂B₂Fe-type Tb₂Ni₂Sn and Dy₂Ni₂Sn compounds, cylindrical BN crucibles (BNP GmbH, HeBoSint® P100, Germany) with a fitting BN plate were filled with the carefully milled precursor compounds. The high-pressure and high-temperature experiments took place in a modified Walker-type module in combination with a 1,000-ton press (both devices from the Voggenreiter, Mainleus, Germany). As pressure medium, precast MgO octahedra (Ceramic Substrates & Components, Isle of Wight, UK) with edge lengths of 18 mm were applied. Eight WC cubes (ha 7 % Co, Hawedia, Marklkofen, Germany) with truncation edge lengths of 11 mm compressed the octahedra. Further information on the construction of the assemblies is given in Ref. [17].

The samples were compressed up to 8 GPa in 3.5 h, then heated to 1,470 K within 15 min and kept there for another 30 min. Afterwards, the samples were cooled down to 1,370 K within 30 min, followed by a tempering period of 120 min with an accompanied decrease of temperature down to 1,170 K. Finally, the samples were quenched to room temperature by switching off the heating. The decompression of the assembly required 10.5 h. The recovered MgO octahedra were broken apart and the samples were carefully separated from the surrounding BN crucible. Polycrystalline samples are gray with metallic lustre and stable in air over months.

Scanning electron microscopy

The HP-Tb₂Ni₂Sn and HP-Dy₂Ni₂Sn single crystals investigated on the diffractometers were analyzed using a Zeiss EVO[®] MA10 scanning electron microscope in variable pressure mode with TbF₃, DyF₃, Ni, and Sn as standards. No impurity elements heavier than sodium (detection limit of the instrument) were observed. The experimentally determined compositions were close to the ideal ones. The extremely irregularly shaped crystal surfaces hampered determination of absolute values.

X-ray diffraction data

The normal-pressure (NP) and high-pressure (HP) RE₂Ni₂Sn samples were characterized by powder X-ray diffraction on a Guinier camera (image plate system, Fujifilm, BAS-1800, Cu K α ₁ radiation and α -quartz ($a = 491.30$ pm, $c = 540.46$ pm) as an internal standard). The lattice parameters (Table 1) were obtained from least-squares refinements. The correct indexing of the patterns was confirmed by intensity calculations [18].

Single crystals of HP-Tb₂Ni₂Sn and HP-Dy₂Ni₂Sn were selected from the HP-HT treated samples by mechanical fragmentation. They were glued to thin quartz fibers using bees wax and their quality was checked by Laue photographs on a Buerger camera (white molybdenum radiation, image plate technique, Fujifilm, BAS-1800). The HP-Tb₂Ni₂Sn data set was collected at room temperature by use of a Stoe IPDS-II image plate system (graphite monochromatized Mo radiation; $\lambda = 71.073$ pm) in

oscillation mode. The HP-Dy₂Ni₂Sn crystal was measured on a Stoe StadiVari equipped with a Mo microfocus source and a Pilatus 100 K detector with a hybrid-pixel-sensor. Numerical absorption corrections were applied to the data sets. All relevant crystallographic data and details of the data collections and evaluations are listed in Table 2.

Further information on the structure refinements is available. Details may be obtained from Fachinformationszentrum Karlsruhe, D-76344 Eggenstein-Leopoldshafen (Germany), by quoting the registry nos. CSD-427285 (TbNiSn), CSD-427284 (DyNiSn), CSD-427282 (Tb₂Ni₂Sn), and CSD-427283 (Dy₂Ni₂Sn).

Acknowledgments This work was financially supported by the Deutsche Forschungsgemeinschaft.

References

1. Heying B, Rodewald UC, Chevalier B, Pöttgen R (2013) *Z Naturforsch* 68b:10
2. Rossi D, Marazza R, Ferro R (1985) *J Less Common Met* 107:99
3. Riecken JF, Heymann G, Hermes W, Rodewald UC, Hoffmann R-D, Huppertz H, Pöttgen R (2008) *Z Naturforsch* 63b:695
4. Sebastian CP, Heymann G, Heying B, Rodewald UC, Huppertz H, Pöttgen R (2007) *Z Anorg Allg Chem* 633:1551
5. Sheldrick GM (1997) SHELXL-97, Program for crystal structure refinement. University of Göttingen, Germany
6. Sheldrick GM (2008) *Acta Crystallogr A* 64:112
7. Dwight AE (1983) *J Less Common Met* 93:411
8. Skolozdra RV, Koretskaya OE, Gorelenko YK (1984) *Inorg Mater* 20:520
9. Yartys VA, Denys RV, Isnard O, Delaplane RG, Svedlindh P, Buschow KHJ (2007) *J Magn Magn Mater* 311:639
10. Emsley J (1999) *The elements*. Oxford University Press, Oxford
11. Lukachuk M, Pöttgen R (2003) *Z Kristallogr* 218:767
12. Pielhofer F, Rothballer J, Peter P, Yan W, Schappacher FM, Pöttgen R, Weihrich R (2014) *Z Anorg Allg Chem* 640:286
13. Hoffmann R-D, Pöttgen R (2001) *Z Kristallogr* 216:127
14. Nuspl G, Polborn K, Evers J, Landrum GA, Hoffmann R (1996) *Inorg Chem* 35:6922
15. Parthé E, Gelato L, Chabot B, Penzo M, Cenzual K, Gladyshevskii R (1993) TYPIX—standardized data and crystal chemical characterization of inorganic structure types. In: *Gmelin handbook of inorganic and organometallic chemistry*, 8th edn. Springer, Berlin
16. Pöttgen R, Gulden T, Simon A (1999) *GIT Labor Fachz* 43:133
17. Huppertz H (2004) *Z Kristallogr* 219:330
18. Yvon K, Jeitschko W, Parthé E (1977) *J Appl Crystallogr* 10:73